Revision 1

Hydrokenomicrolite, $(\square,H_2O)_2Ta_2(O,OH)_6(H_2O)$, a new microlite-group mineral from Volta Grande pegmatite, Nazareno, Minas Gerais, Brazil.

Marcelo B. de Andrade [1,*]
Daniel Atencio [2],
Nikita V. Chukanov[3],
Javier Ellena [1].

[1]Departamento de Física e Informática, Instituto de Física de São Carlos, Universidade de São Paulo, Caixa Postal 369, 13560-970 São Carlos, SP, Brazil
[2]Departamento de Mineralogia e Geotectônica, Instituto de Geociências, Universidade de São Paulo, Rua do Lago 562, 05508-080 São Paulo, SP, Brazil
[3]Institute of Problems of Chemical Physics, Russian Academy of Sciences, Chernogolovka, Moscow Region 142432, Russia
* Present address: Department of Geosciences, University of Arizona, 1040 East 4th Street, Tucson, Arizona 85721, U.S.A. E-mail: mabadean@terra.com.br

Revision 1

ABSTRACT

Hydrokenomicrolite, $(\square,H_2O)_2Ta_2(O,OH)_6(H_2O)$ or ideally $\square_2Ta_2[O_4(OH)_2](H_2O)$, is a new microlite-group mineral approved by the CNMNC (IMA 2011-103). It occurs as an accessory mineral in the Volta Grande pegmatite, Nazareno, Minas Gerais, Brazil. Associated minerals are: microcline, albite, quartz, muscovite, spodumene, "lepidolite", cassiterite, tantalite-(Mn), monazite-(Ce), fluorite, "apatite", beryl, "garnet", epidote, magnetite, gahnite, zircon, "tourmaline", bityite, and other microlite-group minerals under study. Hydrokenomicrolite occurs as euhedral octahedral crystals, occasionally modified by rhombododecahedra, untwinned, from 0.2 to 1.5 mm in size. The crystals are pinkish brown and translucent; the streak is white, and the luster is adamantine to resinous. It is non-fluorescent under ultraviolet light. Mohs' hardness is 4½ - 5, tenacity is brittle. Cleavage is not observed; fracture is conchoidal. The calculated density is 6.666 g/cm^3. The mineral is isotropic, $n_{calc.} = 2.055$. The infra-red spectrum contains bands of O-H stretching vibrations and H-O-H bending vibrations of H_2O molecules. The chemical composition (n = 3) is (by wavelength-dispersive spectroscopy (WDS), H_2O calculated from crystal structure analysis, wt.%): CaO 0.12, MnO 0.27, SrO 4.88, BaO 8.63, PbO 0.52, La_2O_3 0.52, Ce_2O_3 0.49, Nd_2O_3 0.55, Bi_2O_3 0.57, UO_2 4.54, TiO_2 0.18, SnO_2 2.60, Nb_2O_5 2.18, Ta_2O_5 66.33, SiO_2 0.46, Cs_2O 0.67, H_2O 4.84, total 98.35. The empirical formula, based on 2 cations at the B site, is $[\square_{0.71}(H_2O)_{0.48}Ba_{0.33}Sr_{0.27}U_{0.10}Mn_{0.02}Nd_{0.02}Ce_{0.02}La_{0.02}Ca_{0.01}Bi_{0.01}Pb_{0.01}]_{\Sigma 2.00}(Ta_{1.75}Nb_{0.10}Sn_{0.10}Si_{0.04}Ti_{0.01})_{\Sigma=2.00}[(O_{5.77}(OH)_{0.23}]_{\Sigma 6.00}[(H_2O)_{0.97}Cs_{0.03}]_{\Sigma 1.00}$. The strongest eight X-ray powder-diffraction lines [*d* in Å(*I*)(*hkl*)] are: 6.112(86)(111), 3.191(52)(311), 3.052(100)(222), 2.642(28)(400), 2.035(11)(511)(333), 1.869(29)(440), 1.788(10)(531), and 1.594(24)(622).The crystal structure refinement ($R_1 = 0.0363$) gave the following data: cubic,

Revision 1

$Fd\bar{3}m$, a = 10.454(1) Å, V = 1142.5(2) Å^3, Z = 8. The Ta(O,OH)$_6$ octahedra are linked through all vertices. The refinement results and the approximate empirical bond-valences sums for the positions *A* (1.0 v.u.) and *Y*′ (0.5 v.u.), compared to valence calculations from electron microprobe analysis (EMPA) and ranges expected for H_2O molecules, confirm the presence of H_2O at the *A* (16*d*) site and displaced from the *Y*(8*b*) to the *Y*′(32*e*) position. The mineral is characterized by H_2O dominance at the *Y* site, vacancy dominance at the *A* site, and Ta dominance at the *B* site.

Keywords: hydrokenomicrolite, new mineral, Volta Grande pegmatite, Nazareno, Minas Gerais, Brazil, pyrochlore supergroup, microlite group, crystal structure.

INTRODUCTION

Hydrokenomicrolite, $(\square,H_2O)_2Ta_2(O,OH)_6(H_2O)$ or ideally $\square_2Ta_2[O_4(OH)_2](H_2O)$, from Volta Grande pegmatite, Nazareno, Minas Gerais, Brazil, is a new mineral (IMA 2011-103) named according to the nomenclature system for the pyrochlore supergroup of minerals approved by IMA-CNMNC (Atencio et al. 2010). The general formula of the pyrochlore-supergroup minerals is $A_{2-m}B_2X_{6-w}Y_{1-n}$, where m = 0 to 1.7, w = 0 to 0.7, n = 0 to 1 (Lumpkin and Ewing 1995). In hydrokenomicrolite, the *A* site is dominated by vacancies, the *B* site is dominated by Ta, and the *Y* site is dominated by H_2O. The discredited mineral species "bariomicrolite" (Hogarth 1977), identical with "rijkeboerite" (van der Veen 1963), is too poor in Ba to correspond to the name "bariomicrolite". It apparently has a vacancy at the dominant *A* position and H_2O as a predominant component at the *Y* position, and as such is also probably hydrokenomicrolite. The "bariomicrolite" studied by Beurlen et al. (2005) is

Revision 1

probably also hydrokenomicrolite (Atencio et al. 2010). Type material is deposited in the collections of the Museu de Geociências, Instituto de Geociências, Universidade de São Paulo, Rua do Lago, 562, 05508-080 São Paulo, São Paulo, Brazil, registration number DR725.

OCCURRENCE

The mineral occurs as an accessory phase in the Volta Grande pegmatite (21°10'08.6"S 44°36'01.3"W), Nazareno, Minas Gerais, Brazil, and the associated minerals are: microcline, albite, quartz, muscovite, spodumene, "lepidolite", cassiterite, tantalite-(Mn), monazite-(Ce), fluorite, "apatite", beryl, "garnet", epidote, magnetite, gahnite, zircon, "tourmaline", bityite, and other microlite-group minerals under study (Heinrich 1964, Francesconi 1972, Lagache and Quéméneur 1997). The hydrokenomicrolite crystals were collected in a heavy minerals concentrate, so the paragenetic position can not be established. Other crystals of different colors, also corresponding to microlite group minerals occur in the same concentrate. Some of these crystals are formed by the association between Ca-Na-dominant microlite (under study) and hydrokenomicrolite, which may suggest that hydrokenomicrolite is an alteration product of Ca-Na-dominant microlite. The crystals used for characterization of hydrokenomicrolite, however, are homogeneous, not containing, therefore, association with other species. The pegmatite belongs to the Sn-Ta-rich São João del Rei Pegmatite Province. The Volta Grande granitic pegmatite is associated with Transamazonian granites (Early Proterozoic) hosted by the Archean greenstone belt of the Rio das Mortes Valley, which is situated at the southern border of the São Francisco Craton, in Minas Gerais, Brazil (Lagache and Quéméneur 1997). The pegmatite bodies, which are

Revision 1

usually large (up to 1200 x 40 m), show a dominant intermediate zone containing spodumene, microcline, albite and quartz, with an irregular border of an aplitic facies surrounded by an extensive metasomatic aureole with "zinnwaldite", phlogopite and holmquistite. The spodumene-rich core zone is continuous or segmented, and also contains lenses of "lepidolite". The main rock type that hosts the pegmatite is an amphibole schist. This pegmatite is characterized by their high Rb and Li content (Lagache and Quéméneur 1997).

HABIT AND PHYSICAL PROPERTIES

Hydrokenomicrolite occurs as octahedra, occasionally modified by rhombododecahedra, untwinned, from 0.2 to 1.5 mm in size (Figure 1). The crystals are pinkish brown with a white streak. The luster is adamantine to resinous. The mineral is translucent. It is non-fluorescent under ultraviolet light. Mohs' hardness is 4½ - 5; van der Veen (1963) observed VHN_{100} = 485 to 498 kg mm^{-2} with 3 measurements for "bariomicrolite", a mineral that probably is the same as hydrokenomicrolite. The tenacity is brittle. Cleavage was not observed; fracture is conchoidal. The calculated density is 6.666 g/cm^3 based on the empirical formula and unit-cell parameters obtained from the single-crystal X-ray diffraction data.

The mineral is isotropic. Refractive index calculated from the Gladstone-Dale relationship based on the empirical formula is $n_{calc.}$ = 2.055 (higher than that of available immersion liquids). Van der Veen (1963) observed reflectivity of 12.8 to 13.6, mean 13.2, which is equivalent to n = 2.141 (three measurements in air relative to a glass standard with a reflectivity of 8.3%, refractive index 1.809, for "bariomicrolite" (see comments for "bariomicrolite" above).

Revision 1

INFRARED DATA

The infrared (IR) absorption spectrum of hydrokenomicrolite (Figure 2) was obtained for a powdered sample (mixed with anhydrous KBr and pelletized) using BRUKER ALPHA FTIR spectrometer, at the resolution of 4 cm^{-1} and the number of scans equal to 16. A pure KBr-disk was used as a reference sample.

The (IR) spectrum of hydrokenomicrolite contains bands of O-H stretching vibrations (2900-3700 cm^{-1}) and H-O-H bending vibrations of H_2O molecules (1640 and 1620 cm^{-1}). H_2O molecules form hydrogen bonds of different types (from weak to very strong). Weak bands at 890 and 1015 cm^{-1} correspond to stretching vibrations of SiO_4 tetrahedra and/or Ta···O-H bending vibrations. All other bands in the range 360-700 cm^{-1} are due to vibrations of the microlite-type framework.

COMPOSITION OF HYDROKENOMICROLITE

The composition of hydrokenomicrolite was determined using an Oxford INCA Wave 700 electron microprobe (WDS mode, 20 kV, 20 nA, electron beam rastered on the area 300×300 nm^2). H_2O was calculated from the crystal structure data; H_2O determined by gas chromatography of the products obtained by heating at 1200°C is 6.74 wt.%. However, part of this water probably is not a structural component, but is absorbed in macropores. Mean analytical results (n = 3) are given in Table 1. The contents of F, Na, P, S, Cl, K, Fe and Th are below detection limits.

Revision 1

The empirical formula, based on 2 cations at the *B* site is $[\square_{0.71}(H_2O)_{0.48}Ba_{0.33}Sr_{0.27}U_{0.10}Mn_{0.02}Nd_{0.02}Ce_{0.02}La_{0.02}Ca_{0.01}Bi_{0.01}Pb_{0.01}]_{\Sigma 2.00}(Ta_{1.75}Nb_{0.10}Sn_{0.10}Si_{0.04}Ti_{0.01})_{\Sigma=2.00}[O_{5.77}(OH)_{0.23}]_{\Sigma 6.00}[(H_2O)_{0.97}Cs_{0.03}]_{\Sigma 1.00}$. The simplified formula is $(\square,H_2O)_2Ta_2(O,OH)_6(H_2O)$. The only charge-balanced end-member variant of this formula is $\square_2Ta_2[O_4(OH)_2](H_2O)$.

CRYSTAL STRUCTURE DETERMINATION

Powder X-ray diffraction data were obtained using a Siemens D5000 diffractometer equipped with a Göbel mirror and a position-sensitive detector. Data (for Cu*K*α, 40 kV and 40 mA) are given in Table 2. Unit cell parameters refined from powder data (space group $Fd\bar{3}m$) are a = 10.5733(9) Å, V = 1182.0(3) Å^3 and Z = 8.

A pinkish brown crystal with the dimensions $0.197 \times 0.170 \times 0.104$ mm^3 was used for the structural investigation. X-ray diffraction measurements were made with an Enraf–Nonius Kappa-CCD diffractometer with graphite-monochromated Mo*K*α (λ = 0.71073 Å) radiation. Data were collected up to 64^o in 2θ. Final unit-cell parameters are based on 331 reflections with the index ranges $-15 \le h \le 15$, $-11 \le k \le 11$, $-9 \le l \le 9$. The COLLECT program (Enraf-Nonius 1997–2000) was used for data collection, and the integration and scaling of the reflections were performed with the HKL Denzo–Scalepack system of programs (Otwinowski and Minor 1997). Face-indexed numerical absorption corrections were applied (Coppens et al. 1965). The structure was solved using the Patterson method with SHELXS-97 (Sheldrick 2008). The model was refined on the basis of F^2 by full-matrix least-squares procedures. The data obtained are: cubic, space group $Fd\bar{3}m$, a = 10.454(1) Å, V = 1142.4(2) Å^3 and Z = 8. The details concerning data collection procedures, structure

Revision 1

determination and refinement are summarized in Table 3. Other crystallographic data are listed in Tables 4 and 5. More details, including anisotropic ADPs, are in the CIF file (deposit item CSD-424480).

The holotype pyrochlore structures have all atoms occupying special positions (*A* = 16*d*, *B* = 16*c*, *X* = 48*f* and *Y* = 8*b*) in $Fd\bar{3}m$. The *A* position was initially assumed to be *A*(16*d*) and the occupation was constrained by the microprobe obtained compositional data, as $(Ba_{0.33}Sr_{0.27}U_{0.10}Ce_{0.02}La_{0.02}Mn_{0.02}Nd_{0.02}\ Bi_{0.01}Ca_{0.01}Pb_{0.01})_{\Sigma 0.81}$. The *X* and *B* sites were set at full occupancy and *B* was constrained to the value obtained from the compositional data, $(Ta_{1.75}Nb_{0.10}Sn_{0.10}Si_{0.04}Sn_{0.10}Ti_{0.01})_{\Sigma 2.00}$. The *Y* position was refined anisotropically and located at Wyckoff position 8*b*. The Cs content was constrained by microprobe analysis and H_2O presence was also checked. The H_2O occupancy presented positional disorder at 8*b* during refinement while Cs behaved as expected. Attempts to refine *Y′* at 32*e* were done setting anisotropic ADPs. The position 32*e* was modelled partially with an occupation factor of 0.24 as the maximum occupation factor of 8*b* is equal to 1. However, a difference Fourier map showed a large negative maximum, -3.48 e $Å^{-3}$, in the vicinity of the *Y′* site, and a large positive maximum, 2.96 e $Å^{-3}$, in the vicinity of the *Y* site. Thus positions 8*b* and 32*e* were modelled to be fractionally occupied by (Cs, H_2O) and H_2O respectively. Refinement of this model converged to $R_1 = 0.0363$, $wR_2 = 0.1009$. The final model exhibits $(Cs_{0.03}(H_2O)_{0.32})$ at 8*b*, $(H_2O)_{0.65}$ at 32*e* and $(H_2O)_{0.48}$ at 16*d,* and gave a total H_2O content in the mineral of 1.55 *pfu* = (0.48 + 0.97 *pfu*). Charge balance was maintained by replacing O by OH at the *X*(48*f*) position, $[(O_{5.77}(OH)_{0.23}]_{\Sigma 6.00}$ (Figures 3 and 4).

The maximum amount of H_2O in the pyrochlore structure is controlled by the cation occupancy of the *A* site; the maximum H_2O content ranges from 1.00 H_2O *pfu* for ideal pyrochlores (two *A* cations *pfu, i.e.*, *m* = 0) to 1.75 H_2O *pfu* for *A*-deficient pyrochlores (no *A* cations, *i.e.*, *m* = 2) (Ercit et al. 1994). Low *A* site cation content, high displacement

Revision 1

parameters for the *Y* site constituents, and the site splitting sometimes observed for the *Y* site indicate that the "O" on the *Y* sites can be H_2O. Ercit et al. (1994) found that H_2O molecules were actually displaced away from the ideal 8*b Y* sites, and partially occupied higher-multiplicity positions nearby. Displacements were by 0.57 Å along approximately <112> directions to 96*g Y*′, or a similar distance along <111> to 32*e Y*″-positions. A 192*i* position (*Y*‴) very close to *Y*′ was also located by Philippo et al. (1995). Such displacements allow optimal distances between *A* and *Y* site species to be maintained.

For pyrochlore-supergroup minerals AB_2X_6Y, in which *A* and *B* are cations, and *X* and *Y* are anions, there are no stereochemical constraints for the maximum occupancies of the *A* and *Y* sites. However, for pyrochlore-supergroup minerals with H_2O in both the *A* and *Y* sites, the maximum occupancies of both sites are limited owing to the short separation between the ideal *A* and *Y* sites, which is in the neighborhood of 2.3 Å (Ercit et al. 1994). Partial occupancy of the *A* site and positional disorder of H_2O at *A* and *Y* sites permit acceptable O...O separations for neighbouring H_2O groups in pyrochlore. Ercit et al. (1994) found that positional disorder can result in eight fractionally occupied *A*′ sites around each *A* site, displaced from the ideal site by about 0.11 Å along <111> directions. Five of the eight are too close to the offset *Y*′ and *Y*″ positions to represent stable O...O separations for H_2O groups; however, three of the eight subsites are sufficiently distant to correspond to realistic intermolecular distances (averaging 2.74 Å). Philippo et al. (1995) reported a different displacement scheme, in which H_2O partially occupied *A*″-sites displaced from *A* by 0.75 Å along <100>. For synthetic cation-free *A*-site pyrochlore, the maximum H_2O content *pfu* may be limited by the need to avoid close H_2O...H_2O distances. If there is one H_2O group *pfu* in the *Y* site, then there can be only 3/8 H_2O groups in the *A* site. This constraint translates to a maximum of 1.75 H_2O *pfu* for *A* cation-free pyrochlore. Previous refinements of the structures of H_2O-bearing pyrochlore-supergroup minerals (*e.g.*, Groult et al. 1982) have

Revision 1

shown the presence of H_2O only in the vicinity of the *Y* site. As no synthetic or natural pyrochlore has been found with all H_2O ordered at *A*, we presume that the *Y* site and its displaced variants are the preferred locations for H_2O, and that H_2O only enters the *A* sites if *Y* cannot accommodate more H_2O. The maximum amount of H_2O *pfu* in the pyrochlore structure is thus $1 + (3m/8)$ where *m* indicates the vacancy at *A* the site.

The total amount of H_2O in the mineral is insufficient for the predominance of H_2O in the *A* site, but H_2O is predominant in the *Y* and *Y*′ sites (Table 4). Empirical bond-valences (Table 5) were calculated using the parameters published by Brown and Altermatt (1985). These values agree with the composition of the *X* anion site chosen to balance the chemical formula and confirm the presence of molecular H_2O at the *Y*′ site. The final refinement is consistent with a cubic $Fd\bar{3}m$ structure and the charge-balanced empirical formula is $[\square_{0.71}(H_2O)_{0.48}(Ba_{0.33}Sr_{0.27}U_{0.10}Ce_{0.02}La_{0.02}Mn_{0.02}Nd_{0.02}Bi_{0.01}Ca_{0.01}Pb_{0.01})_{0.81}]_{\Sigma 2.00}(Ta_{1.75}Nb_{0.10}Sn_{0.10}Si_{0.04}Sn_{0.10}Ti_{0.01})_{\Sigma=2.00}[O_{5.77}(OH)_{0.23}]_{\Sigma 6.00}[Cs_{0,03}(H_2O)_{0,97}]_{\Sigma 1.00}$.

Regardless of the absence of tetrahedral sites suitable for Si incorporation in the pyrochlore structure, octahedral Si is possible. The occurrence of Si in pyrochlore group minerals was discussed by Atencio et al. (2010). Perhaps hydrokenomicrolite could be an example of a mineral with mixed occupancies of a key domain. Unlike sites *sensu stricto*, domains can be defined as microregions in the unit cell that can host a number of alternative sites having, in a general case, different coordination numbers, as in eudialyte-group minerals (Nomura et al. 2010). Thus, an NbO_6 octahedron would be "replaced" by a SiO_4 tetrahedron. When Nb is in the microregion, the coordination number would be 6 and when Si is in the microregion, it would be 4.

Other argument in favour of the possible presence of SiO_4 tetrahedra in hydrokenomicrolite comes from the fact that there are several minerals (titano- and niobosilicates, or, more precisely, oxosilicates) whose crystal structures are regular

interstratifications of pyrochlore-type and silicate modules (blocks). The best known example is natrokomarovite, but several other minerals have such structures as well (*e.g.*, diversilite-(Ce), ilímaussite-(Ce), fersmanite) (Pekov et al. 2004). By analogy, one can suppose that pyrochlore-supergroup minerals can contain, locally, two- or three-dimensional structural defects irregularly distributed within individual crystals. Such "block isomorphism" is not a rare phenomenon for minerals whose crystal structures are based on frameworks with relatively low density (cf. two local situations in the unit cell of manganoeudialyte (Nomura et al. 2010). If this supposition is correct, Si-bearing defects cannot be detected by single-crystal structural analysis. However, high-resolution electron microscopy might be useful to solve this problem.

ACKNOWLEDGEMENTS

We acknowledge FAPESP (processes 2008/04984-7, 2009/09125-5 and 2011/22407-0), CNPq and RFBR (grant no. 11-05-12001-ofi-m-2011) for financial support, and all members of the IMA Commission on New Minerals, Nomenclature and Classification for their helpful suggestions and comments. Thanks are due to Charles H. Lake for critical discussion of the structure refinement procedure during the “ACA Summer Course 2009” (Indiana University of Pennsylvania). We thank Fernando Colombo, Ron Peterson, Roger H. Mitchell, and Joan Carles Melgarejo for their very important comments.

Revision 1

REFERENCES CITED

Atencio, D., Andrade, M.B., Christy A.G., Gieré, R. and Kartashov, P.M. (2010) The pyrochlore supergroup of minerals: nomenclature. Canadian Mineralogist, 48, 673-698.

Beurlen, H., Soares, D.R., Thomas, R., Prado-Borges, L.E. and Castro, C. (2005) Mineral chemistry of tantalate species new in the Borborema Pegmatitic Province, Northeast Brazil. Anais da Academia Brasileira de Ciências, 77, 169-182

Brown, I.D. and Altermatt, D. (1985) Bond-valence parameters obtained from a systematic analysis of the inorganic crystal structure data base. Acta Crystallographica, B41, 244-247.

Coppens, P., Leiserowitz, L. and Rabinovich, D. (1965) Calculation of absorption corrections for camera and diffractometer data. Acta Crystallographica, 18, 1035-1038.

Enraf-Nonius (1997–2000) Collect. Nonius BV, Delft, The Netherlands.

Ercit, T.S., Hawthorne, F.C. and Černý, P. (1994) The structural chemistry of kalipyrochlore, a "hydropyrochlore" Canadian Mineralogist, 32, 415-420.

Francesconi, R. (1972) Pegmatitos da região de São João del Rei – MG. Ph.D thesis, Universidade de São Paulo, São Paulo, Brazil.

Groult, D., Pannetier, J. and Raveau, B. (1982) Neutron diffraction study of the defect pyrochlores $TaWO_{5.5}$, $HTaWO_6$, $H_2Ta_2O_6$, and $HTaWO_6.H_2O$. Journal of Solid State Chemistry, 41, 277-285.

Heinrich, E.W.M. (1964) Tin-tantalum-lithium pegmatites of the São João Del Rei district, Minas Gerais, Brazil. Economic Geology, 59, 982-1002.

Hogarth, D.D. (1977) Classification and nomenclature of the pyrochlore group. American Mineralogist, 62, 403-410.

Revision 1

Lagache, M. and Quéméneur, J. (1997) The Volta Grande pegmatites, Minas Gerais, Brazil: an example of rare-element granitic pegmatites exceptionally enriched in lithium and rubidium. Canadian Mineralogist, 35, 153-165.

Lumpkin, G.R. and Ewing, R.C. (1995) Geochemical alteration of pyrochlore group minerals: pyrochlore subgroup. American Mineralogist, 80, 732-743.

Nomura, S.F., Atencio, D., Chukanov, N.V., Rastsvetaeva, R.K., Coutinho, J.M.V. and Karipidis, T. (2010) Manganoeudialyte, a new mineral from Poços de Caldas, Minas Gerais, Brazil. Zapiski Rossiiskogo Mineralogicheskogo Obshchestva, 139, 35-47.

Otwinowski, Z. and Minor, W. (1997) Processing X-ray diffraction data collected in oscillation mode. In: C.W. Carter, Jr. and R.M. Sweet, eds. Methods in Enzymology, 276, Academic Press, New York, pp. 307-326.

Pekov, I.V., Azarova, Y.V. and Chukanov, N.V. (2004) New data on komarovite series minerals. New Data on Minerals, 39, 5-13.

Philippo, S., Naud, J., Declerq, J.P. and Feneau-Dupont, J. (1995) Structure refinement and X-ray powder diffraction data for kalipyrochlore $(K,Sr,Na,Ca,H_2O)_{2-m}(Nb,Ti)_{2-x}O_{6-w}Y_{1-n}$ with ($0 < m < 0.8$, x ca. 0.2, $w = 0$ and $0.2 < n < 1$). Powder Diffraction, 10, 180-184.

Sheldrick, G.M. (2008) A short history of SHELX. Acta Crystallographica, A64, 112-122.

van der Veen, A.H. (1963) A study of pyrochlore. Verhandelingen van het Koninklijk Nederlands geologisch mijnbouwkundig genootschap, Geologische serie, 22, 1-188.

Figure 1. Hydrokenomicrolite from Nazareno, Minas Gerais, Brazil.

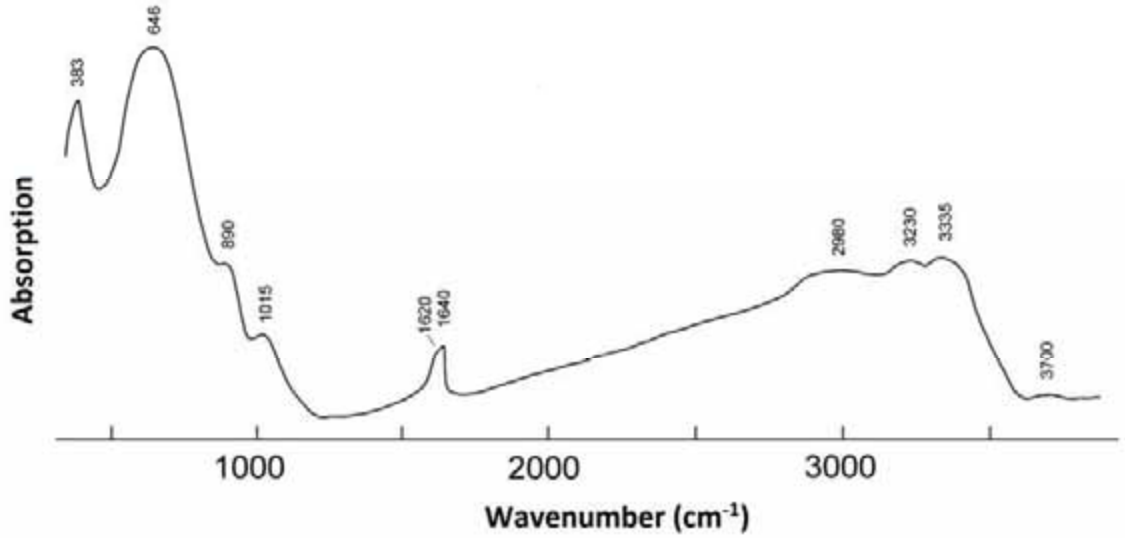

Figure 2. IR spectrum of hydrokenomicrolite

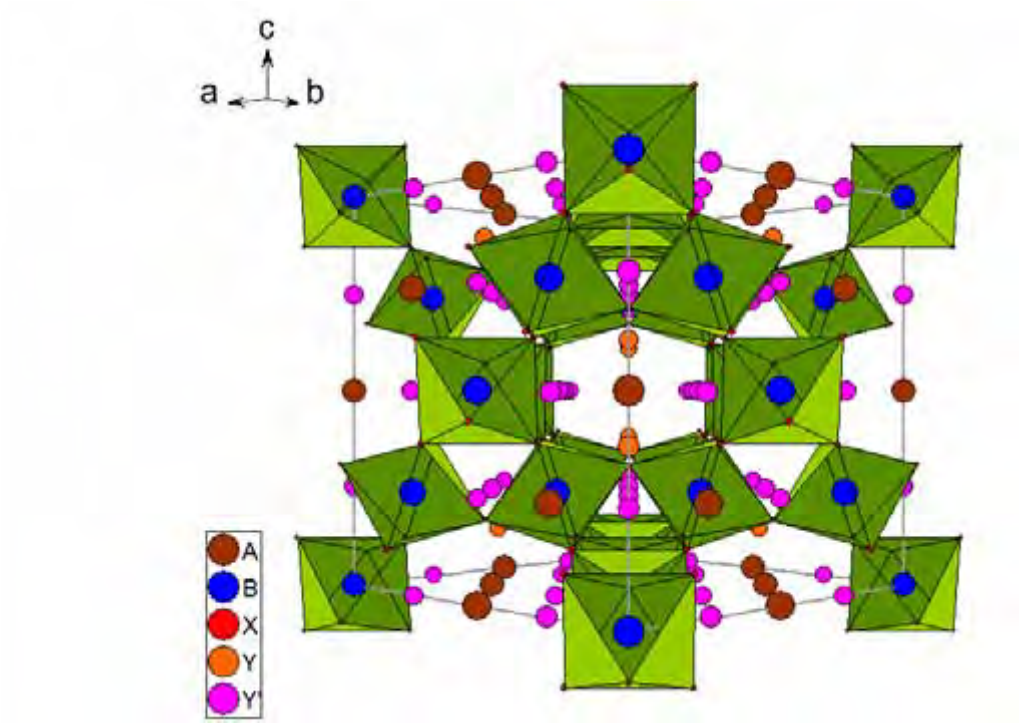

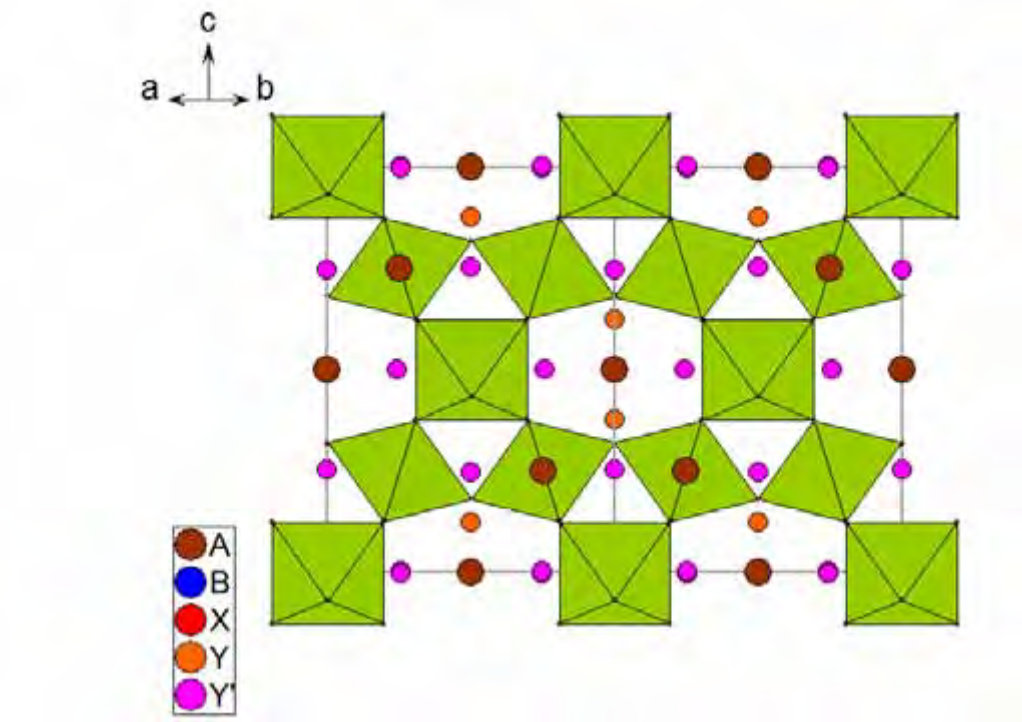

Figure 3 – Hydrokenomicrolite structure

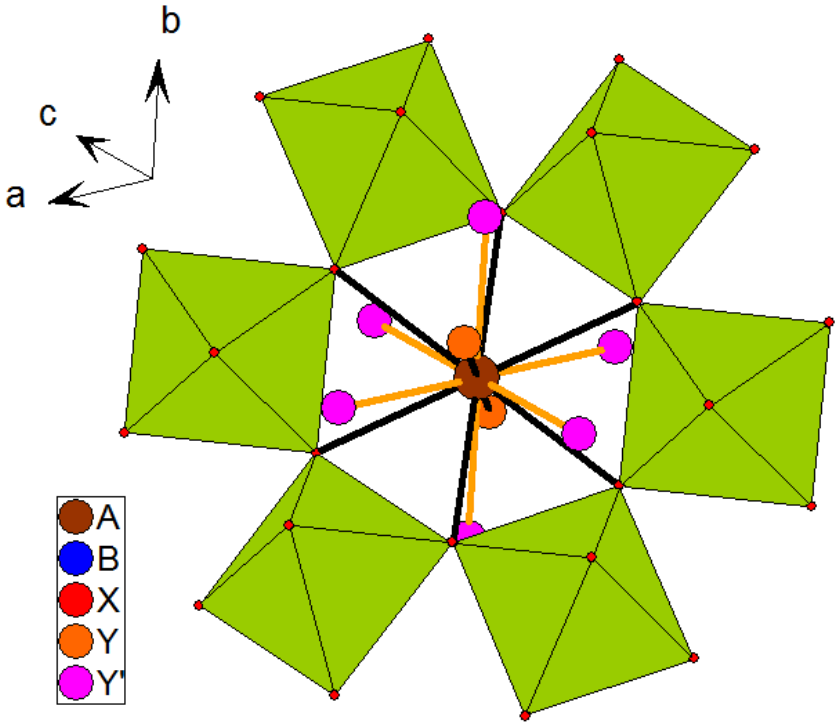

Figure 4 - Relationship between *Y* and *Y*' sites


200 µm

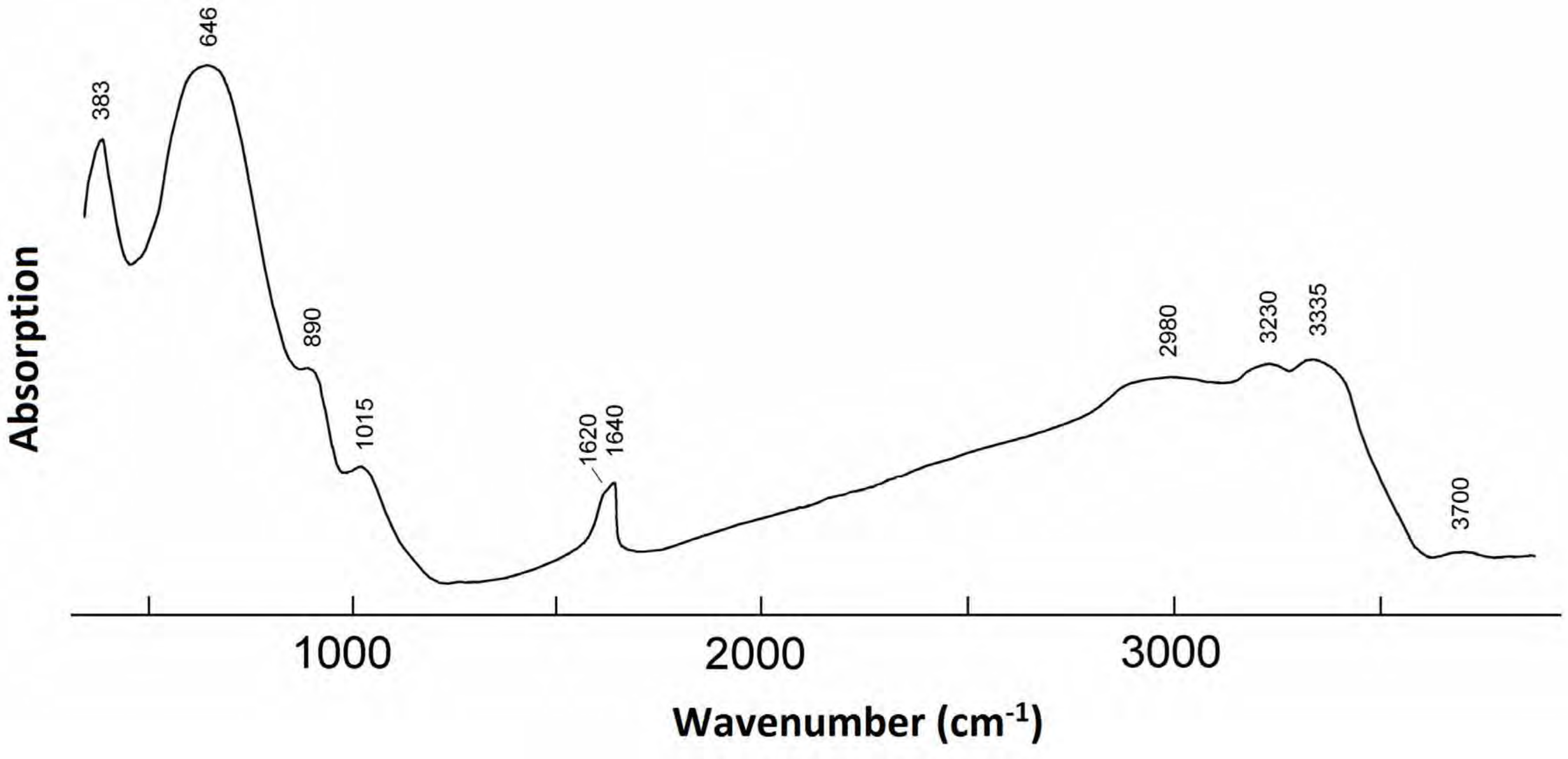
Absorption
383
646
890
1015
1620
1640
2980
3230
3335
3700
1000
2000
3000
Wavenumber (cm-1)

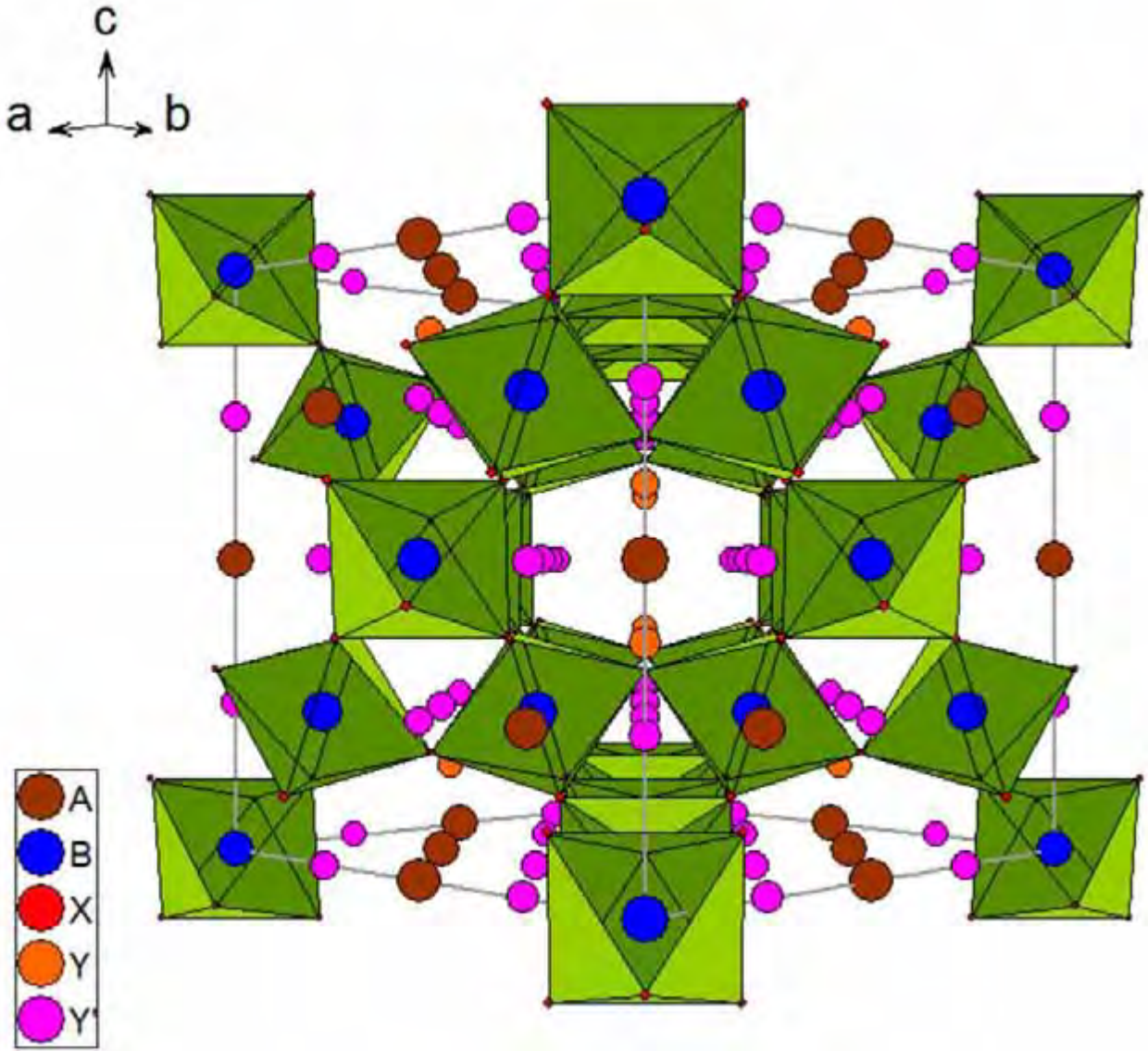
c
a
b
A
B
X
Y
Y'

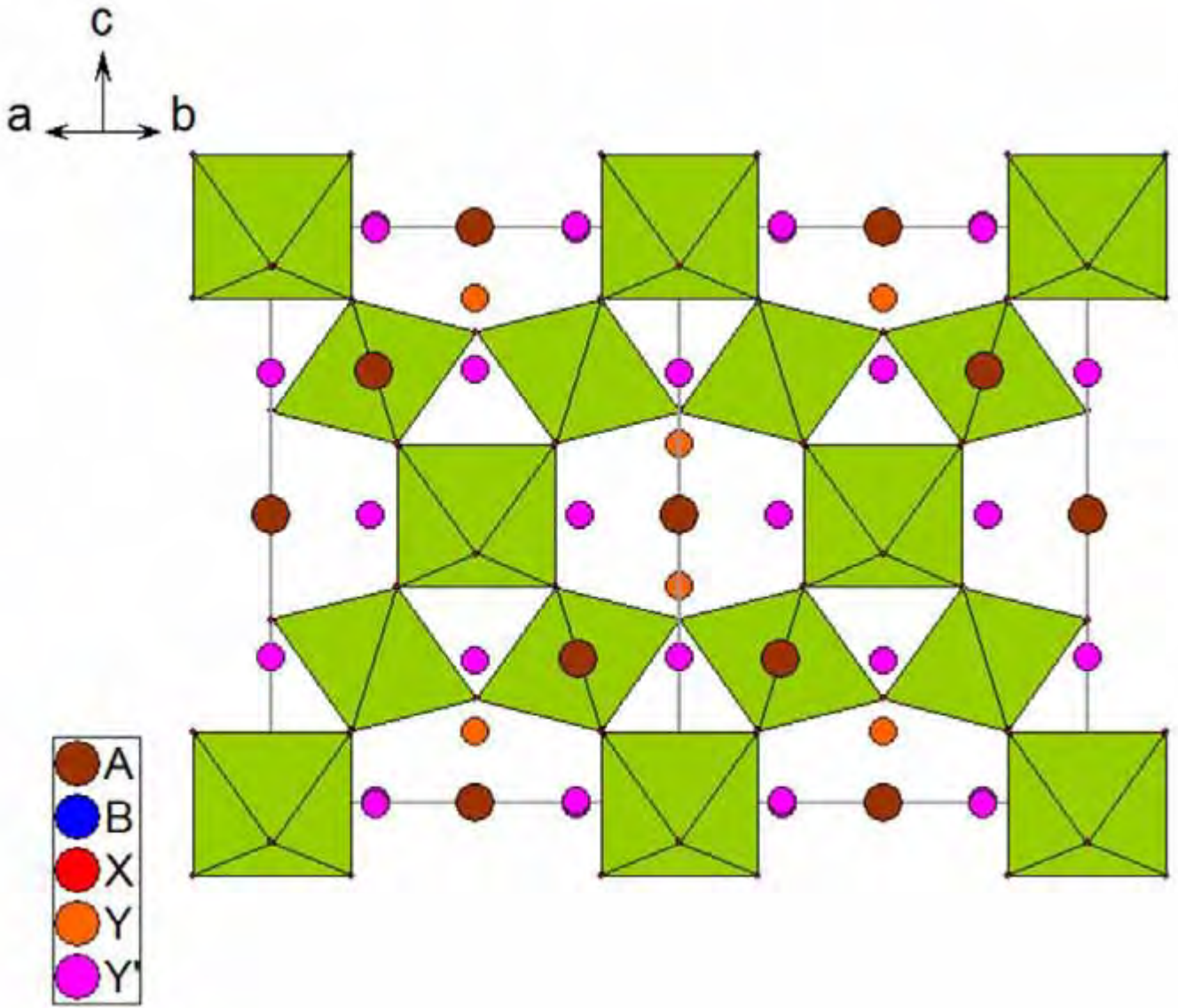
c
a
b
A
B
X
Y
Y'

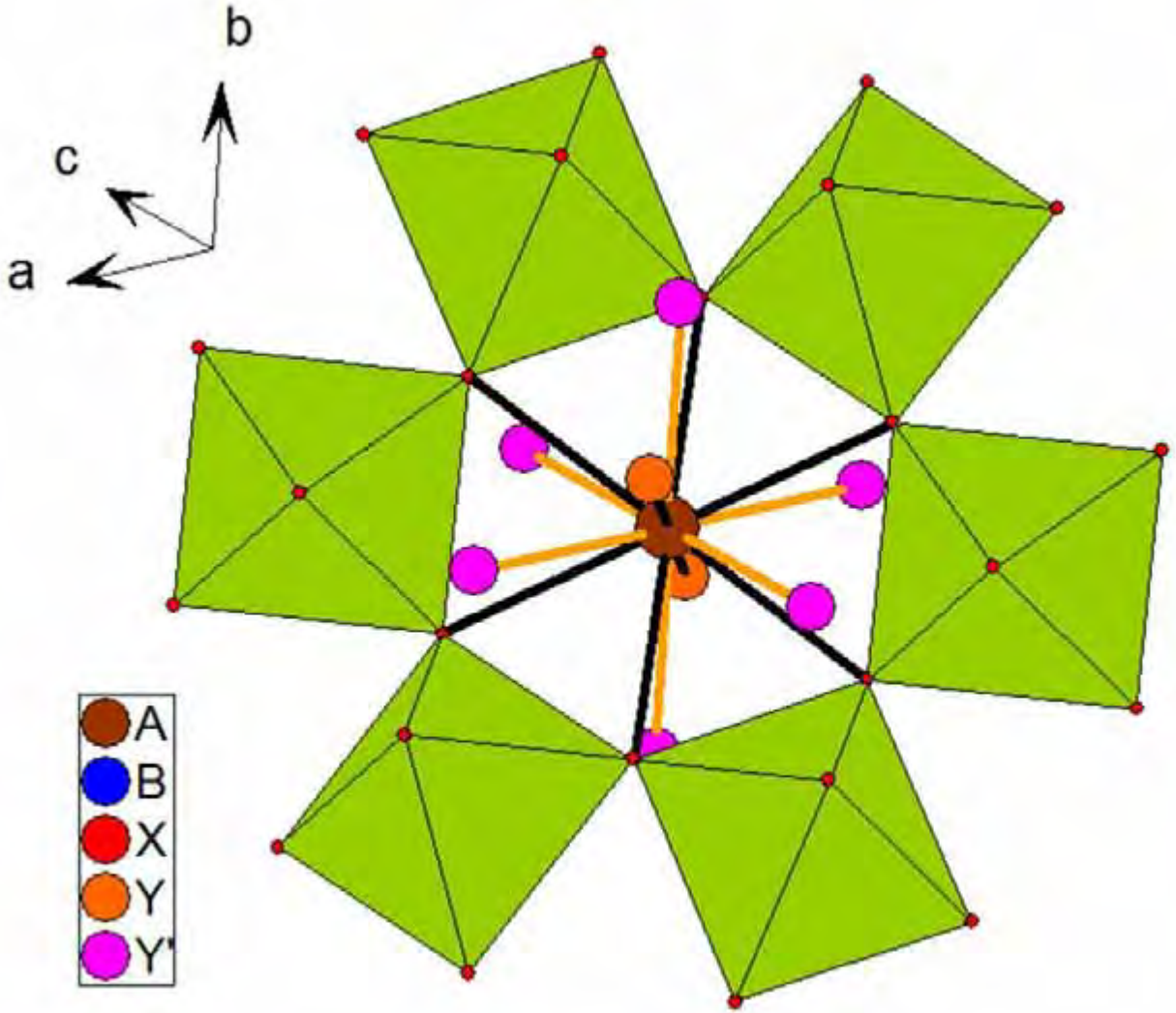
b
c
a
A
B
X
Y
Y'

Table 1. Chemical analyses of hydrokenomicrolite (n = 3).

	wt.%	**Range**	**Microprobe standard**
CaO	0.12	n.d.-0.20	wollastonite
MnO	0.27	0.22-0.36	Mn
SrO	4.88	4.61-5.37	SrF_2
BaO	8.63	8.40-8.83	BaF_2
PbO	0.52	0.39-0.59	PbTe
La_2O_3	0.52	0.50-0.54	$LaPO_4$
Ce_2O_3	0.49	0.37-0.62	$CePO_4$
Nd_2O_3	0.55	0.49-0.62	$NdPO_4$
Bi_2O_3	0.57	0.40-0.74	Bi
UO_2	4.54	3.91-4.88	UO_2
TiO_2	0.18	0.14-0.27	Ti
SnO_2	2.60	2.40-2.98	Sn
Nb_2O_5	2.18	1.71-2.47	Nb
Ta_2O_5	66.33	65.76-67.39	Ta
SiO_2	0.46	n.d.-0.72	SiO_2
Cs_2O	0.67	0.60-0.76	CsCl
H_2O*	4.84		
Total	**98.35**		

* calculated from the structure refinement.

Table 2. X-ray powder-diffraction data for hydrokenomicrolite.

$d_{obs.}$(Å)	$d_{calc.}$(Å)	$I_{obs.}$ (%)	h	k	l
6.112	6.104	86	1	1	1
3.191	3.188	52	3	1	1
3.052	3.052	100	2	2	2
2.642	2.643	28	4	0	0
2.424	2.426	7	3	3	1
2.035	2.035 2.035	11	5 3	1 3	1 3
1.869	1.869	29	4	4	0
1.788	1.787	10	5	3	1
1.613	1.612	7	5	3	3
1.594	1.594	24	6	2	2
1.527	1.526	7	4	4	4
1.480	1.481 1.481	7	7 5	1 5	1 1
1.376	1.377 1.377	6	7 5	3 5	1 3
1.213	1.213	5	6	6	2
1.182	1.182	5	8	4	0

- indexed with a = 10.5733 Å.

Table 3. Crystal data and details of structure refinement

Temperature (K)	293(2)
Crystal color	pinkish brown
Crystal size (mm)	0.197 x 0.170 x 0.104
Formula weight	577.2
Crystal system	Cubic
Space group	$Fd\bar{3}m$ (227)
Unit-cell dimension *a*	10.454(1) Å
Unit-cell volume *V*	1142.4(2) $Å^3$
Z	8
Density (calculated)	6.7 g/cm^3
Absorption coefficient	38.097
F(*000*)	1941
Reflections collected/unique	331/121
Parameters	16 (R_{int} = 0.056)
Goodness-of-fit on F^2	1.191
Final *R* indices [$I > 2\sigma(I)$]	R_1 = 0.0363 , wR_2 = 0.1009
Largest diff. peak and hole	1.75 and -2.16 $e.Å^{-3}$

Table 4. Wyckoff positions, site occupancies, atom coordinates and equivalent isotropic displacement parameters ($Å^2$) in hydrokenomicrolite.

	Wyckoff	Occupancy	x	Y	z	$U_{eq}(Å^2)$
A	16*d*	0.64	1/2	½	1/2	0.0556(17)
B	16*c*	1	0	0	0	0.0306(6)
X	48*f*	1	0.3191(14)	1/8	1/8	0.038(3)
Y	8*b*	0.35	3/8	3/8	3/8	0.051(14)
Y′	32*e*	0.16	0.747(4)	0.747(4)	0.747(4)	0.051(14)

Table 5. Selected bond lengths and bond valences of the refined hydrokenomicrolite structure.

Bond	Bond length	BV (v.u)	Σ	Valence from EMPA
A(16*d*)-*X*(48*f*)	2.644(10)	0.119 (x6)	0.714	
A(16d)-X(8b)	2.2633(2)	0.106 (x2)	0.212	
A(16*d*)-*Y'*(32*e*)	2.59(6)	0.022 (x6)	0.132	
Σ			**1.058**	**1.080**
B(16*c*)-*X*(48*f*)	1.984(5)	0.828 (x6)	4.968	
Σ			**4.968**	**4.926**
X(48*f*)-*A*(16*d*)	2.644(10)	0,119 (x2)	0.238	
X(48*f*)-*B*(16*c*)	1.984(5)	0.807 (x2)	1.614	
Σ			**1.852**	**1.962**
Y(8b)-A(16d)	2.2633(2)	0.106 (x4)	0.424	
Σ			**0.424**	**0.000**
Y'(32*e*)-*A*(16*d*)	2.59(4)	0.022 (x3)	0.066	
Σ			**0.066**	**0.000**